A methodology for testing, characterization and prediction of edge seal performance in PV modules

Kedar Hardikar, **Dan Vitkavage**, **Ajay Saproo** & **Todd Krajewski**, MiaSolé, Santa Clara, California, USA

ABSTRACT

A critical failure mechanism of PV modules is the degradation in performance as a result of exposure to temperature and humidity during a typical product lifetime of over 25 years. The time to failure of a PV module attributable to moisture ingress under given field conditions involves multiple factors, including encapsulant and edge seal moisture barrier performance as well as the degradation rate of particular solar cells when exposed to moisture. The aim of the work presented here is to establish a conservative estimate of field lifetime by examining the time to breakthrough of moisture across the edge seal. Establishing a lifetime model for the edge seal independent of the characteristics of the encapsulant and solar cells facilitates the design optimization of the cells and encapsulant. For the accelerated testing of edge seal materials in standard temperature- and humidity-controlled chambers, a novel test configuration is proposed that is amenable to varying dimensions of the edge seal and is decoupled from encapsulated components. A theoretical framework that accounts for the presence of desiccants is developed for analyzing the moisture ingress performance of the edge seal. Also developed is an approach to analyzing test data from accelerated testing which incorporates temperature dependence of the material properties of the edge seal. The proposed equations and functional forms have been validated by demonstrating fits to experimental test data. These functional forms and equations allow the prediction of edge seal performance in field conditions characterized by historical meteorological data. In the specific case of the edge seal used in certain MiaSolé glass–glass modules, this work has confirmed that the edge seal can prevent moisture ingress well beyond the intended service lifetime in the most aggressive climate conditions evaluated.

Introduction

According to the recently announced first ever US roadmap for CIGS technology [1], this technology is positioned to lead solar efforts in the USA. The degradation in performance of CIGS-based modules due to moisture ingress is a concern and has also been reported as a failure mechanism in c-Si modules [2]. Additionally, the degradation of encapsulated electronic components caused by moisture ingress is a problem in other products, for example those in the consumer electronics industry, where critical components such as electronic displays and IC metallization may be at risk of degraded performance as a result of moisture ingress and corrosion [3,4].

“The degradation in performance of CIGS-based modules due to moisture ingress is a concern.”

There have been several attempts in the past to develop techniques and models to predict the lifetime of PV modules with moisture ingress as a proposed mechanism leading to failures or degradation in performance [5–8]. It is standard practice in the consumer electronics industry to use the Hallberg-Peck relation [9–11] for analyzing the data from reliability testing of IC packages involving temperature and humidity. In all of these scenarios, predicting the time to failure of the product because of moisture ingress hinges upon the convolution of two factors – moisture barrier performance and degradation of the encapsulated components – when exposed to moisture. The third factor involved in these predictions is the development of schemes to model fluctuations in the ambient conditions that the product is subjected to during its lifetime, and relating these variations to the test conditions [5]. The results of a typical experimental scheme are often specific to a particular design or a set of encapsulated components. While such a holistic approach to predicting the reliability of components is necessary, a somewhat different approach – independently examining sealant lifetime – is required, in order to allow an independent optimization of other design elements and component selection.

Fig. 1 shows the typical structure of a glass–glass PV module. In the construction of a glass–glass module there are four main components pertinent to the discussion in this paper. PV cells are encapsulated in the main encapsulant. The structure is laminated between two pieces of glass. Along the periphery of the module between the two glass pieces is an edge seal. In PV modules the encapsulant chosen has additional constraints placed on it, such as transmission of light, and hence one may not be able to choose a material that in itself is an adequate moisture barrier. A common approach to overcome this constraint in PV modules is the use of an edge seal of appropriate width as shown in Fig. 1. The edge seal can have significantly better moisture barrier performance relative to the encapsulant without any constraint with regard to light transmission. Since the use of glass on two sides of the encapsulated cell effectively prevents moisture from directly reaching the encapsulated cell, the primary path for moisture ingress is through the edge seal and then through the main encapsulant via lateral diffusion. The width of the edge seal corresponds to a non-active area of the PV module: a judicious choice of material and width of the edge seal is therefore critical for maximizing the active area of the module while not compromising the moisture barrier performance of the product. One approach to designing and developing PV modules that

(a)

(b)

Figure 1. MiaSolé glass–glass module: (a) Planar view; (b) Cross section representation, with $CoCl_2$ indicator paper used for product level moisture ingress testing.

incorporate edge seals is to co-optimize the edge seal and the components for every design permutation. With the use of such an approach, however, the duration and cost of validation can be prohibitive. The proposed approach of decoupling edge seal validation from other design components allows shorter design cycles.

> "A judicious choice of material and width of the edge seal is critical for maximizing the active area of the module while not compromising the moisture barrier performance of the product."

Typically, the design and materials for an edge seal are arrived at by first selecting a material based on its properties, such as diffusivity, solubility and permeability at different temperature and humidity conditions, which are presumed to be predictive of field performance. This is followed by an assessment of the edge seal performance from product level tests that use manifestations of failure modes, such as corrosion, hydrolysis of plastics, or cell degradation. Such product degradation, which combines edge seal performance with the characteristics of other components, acts as the sensor for moisture ingress. This approach does not provide an independent means of validating the field performance of the edge seal, which is necessary for employing the design approach outlined above.

The measurement techniques that focus on the characterization of material properties often involve sample preparation that may not be representative of how the material is prepared in the end product. Standard moisture permeation testing techniques (i.e. MOCON) have been used to carry out basic comparisons of sealant properties [12]. However, this testing suffers from the need to use a defect-free self-supporting film or a carrier film. Both of these issues result in either longer test times (due to sample thickness) or convoluting factors from the support. Moreover, the material used in these tests may not be subjected to exactly the same manufacturing conditions that are seen during mass production.

Another factor to consider is the test time required to see the device degradation in a typical module assembly. For certain MiaSolé production module assemblies subjected to some of the highest widely accepted acceleration factors (85°C/85%RH), it requires well in excess of 8000hrs to see a discernible signal. In order to overcome this issue, the test structure dimensions should enable a shorter time to detect a signal in a manner that can be scaled to product-level dimensions, but the scaling methodology adopted would need to be validated. It is therefore desirable to have a framework of testing, analysis and modelling such that data, from tests carried out in standard environmental chambers and with the material in a form representative of end product use, are directly translatable to lifetime estimation.

In summary, the three main objectives of this paper are:

1. To develop a theoretical framework which facilitates the analysis of moisture ingress data obtained in environmental chamber testing in a manner that enables the prediction of edge seal lifetime in field conditions.

2. To provide a relatively inexpensive test configuration to assess moisture barrier performance of the edge seal material in its end product form and decoupled from other components.

3. To provide functional forms that translate these test results to field conditions characterized by meteorological data. The methodology presented in this paper maintains consistency between the analysis of test results and the analysis of weather conditions to which the product is subjected during its lifetime.

The organization of this paper is as follows. First, a theoretical framework under which the testing and analysis is performed will be developed. The objective of this section is to lay out the framework in order to conjecture certain functional forms for the time to failure of the edge seal material being tested and use them for predicting the field performance. Next, the test sample and experimental set-up are discussed in detail, followed by the experimental data. After an analysis of the experimental data, the discussion moves on to the validation of the use of the proposed functional forms. Finally, the results are used for predicting the field performance of a particular edge seal, employed in certain MiaSolé products, in selected locations around the globe.

Theoretical background

The diffusion of moisture through a barrier material is a process which involves adsorption of moisture on the exposed surface of the edge seal followed by diffusion of moisture through the edge seal. The primary driving force for any diffusion process is the concentration gradient of the diffusing species (Fick's Law). Typically the maximum concentration of moisture at the exposed surface of the edge seal is a function of the solubility of the material. The propagation of moisture through the edge seal is a function of the diffusivity of the material. Expected variation of the diffusion time and length scales can be obtained by considering the 1D diffusion equation

$$\frac{\partial C}{\partial t} = D\frac{\partial^2 C}{\partial x^2} \tag{1}$$

where C = moisture concentration, D = diffusivity of the material, t = time and x = distance from the exposed edge.

By merely considering the dimensions of the quantities involved in Equation 1, it can be shown that the extent to which the moisture penetrates x^* in time t has a $\sqrt{t}$ dependence, i.e. $x^* \propto \sqrt{t}$. It also follows that the time t^* for moisture to penetrate a distance l has the dependence given by $t^* \propto l^2/D$. Formal analytical solutions to the diffusion equation for various boundary conditions can be found in Crank [13]. For an unbounded medium (1D) with concentration at the edge given by $C(0, t) = C_0$, the solution is given by

$$C(x,t) = C_0\left[1 - erf\left(\frac{x}{2\sqrt{Dt}}\right)\right] \tag{2}$$

where erf denotes the error function. This implies that when edge seal configurations of different widths x are tested to 'failure' (defined by moisture penetration), the expected variation of the time to failure (t_f) is

$$t_f = Ax^2; \quad A \propto \frac{1}{D} \tag{3}$$

In PV modules it is customary to use edge seal materials which have desiccants embedded in them. The role of the desiccant is to consume moisture migrating through the edge seal by a chemical reaction, thereby further delaying the time to initial moisture breakthrough. Assuming that the desiccant is uniformly loaded throughout the material, the amount of moisture consumed before the moisture penetrates through the entire width of the edge seal is proportional to the width of the edge seal. Hence, the additional delay because of the presence of desiccant is expected to be proportional to the width of the edge seal. Thus, in the presence of desiccant, the expected variation of the time to failure for an edge seal (as a function of width x) is

$$t_f = Ax^2 + Bx \tag{4}$$

where A and B are constants to be determined. Since the prediction of edge seal performance in the field is of particular interest, it is necessary to consider how constants A and B in Equation 4 might vary with changes in ambient conditions. The following discussion is intended to develop likely functional forms for the constants A and B; the functional forms that are conjectured here are later validated by experimental data.

First, it is observed that the 1D diffusion equation (Equation 1) in an unbounded medium with concentration C_0 at the free edge results in non-zero concentration in the *entire* domain, even at infinitesimal time increments, because of the parabolic nature of the partial differential equation. Hence, the definition of 'moisture penetration' is really dependent on the identification of a threshold value $C = C^*$ at which the penetration is considered a failure. In practice, C^* corresponds to the concentration required for the sensor to detect the moisture past the edge seal, with the underlying assumption that the sensor threshold is representative of the failure threshold. Using Equation 2, the time to failure (t_f) for a diffusion-dominated process (not taking into account desiccant) is expected to have a functional form consistent with

$$C^* = C_0\left[1 - erf\left(\frac{x}{2\sqrt{Dt_f}}\right)\right] \tag{5}$$

Rewriting Equation 5 to solve for time to failure yields

$$t_f = \frac{x^2}{4D\left[erf^{-1}\left(1 - \frac{C^*}{C_0}\right)\right]^2} \tag{6}$$

The quantity in parentheses denotes the inverse of the error function. Reconciling Equation 6 with Equation 3 suggests that in Equation 4 we should expect

$$A \propto \frac{1}{D\left[erf^{-1}\left(1 - \frac{C^*}{C_0}\right)\right]^2} \tag{7}$$

To identify a suitable functional form for analysis of experimental data it is first noted that the diffusivity D is expected to have an Arrhenius variation with temperature [4,13]

$$D = D_0 \exp\left(-\frac{\varepsilon_a}{kT}\right) \tag{8}$$

where D_0 is the reference value of diffusivity, ε_a is the activation energy and T is absolute temperature. Hence, the constant A is expected to have an exponential variation $A \propto \exp(\gamma/T)$, where γ is treated as a fit parameter.

Now let $\lambda = C^*/C_0$. Fig. 2 shows a plot of the function $f(\lambda)$ and suggests a corresponding linear approximation for $f(\lambda)$ given by

$$f(\lambda) = \frac{1}{\left[erf^{-1}(1-\lambda)\right]^2} \approx \alpha_1 + \beta_1\lambda \tag{9}$$

where $\lambda = C^*/C_0$. The linear approximation is representative of $f(\lambda)$, particularly at lower values of $\lambda = C^*/C_0$. For the detection of moisture ingress, one would indeed expect $\lambda = C^*/C_0$ to be sufficiently small. In any case, for a particular detection threshold an appropriate linearization that is representative of the function in the neighbourhood can be chosen. Combining Equations 7–9 it is proposed that constant A in Equation 4 for various conditions should have a functional form given by

$$A = \left(\alpha + \frac{\beta}{C_0}\right)\exp\left(\frac{\gamma}{T}\right) \tag{10}$$

where C_0 is the edge concentration. The edge concentration, in turn, depends on the absolute humidity for given ambient conditions and the solubility of the material. Since the constants β and γ are to be determined on the basis of experimental data, C_0 may be used as absolute humidity for given ambient or test conditions. Factors relating to the absolute humidity and edge concentration can be absorbed in β, and the exponential term determined by the fit. Note that, on the basis of this choice, the fit parameter γ may not represent the activation energy ε_a for diffusion alone. If necessary, this functional form can always be maintained by means of suitable changes to the fit parameter definitions if relative humidity is used to characterize edge concentration rather than absolute humidity. As will be shown later, the proposed functional form in Equation 10 demonstrates excellent agreement with the experimental data. In conventional techniques such as the use of the Hallberg-Peck relation [9], it is customary to use relative humidity for the analysis of moisture ingress instead of absolute humidity. Absolute humidity is related to temperature as well as to relative humidity, and hence, as far as analysis of experimental data is concerned, the functional form in Equation 10 is justified as long as it is validated by an appropriate fit to experimental data. It is the authors' view that the distinguishing factor in using the functional form in Equation 10 is that it is based on an analytical solution to the diffusion equation and is an approximation to the solution derived on a rational basis.

Note that constant B in Equation 4 is dependent on the reaction rate for the reaction between the moisture and the desiccant. Compared with the time scale of moisture diffusion, the reaction is expected to be instantaneous. The constant B may therefore be assumed to depend only on C_0, and the proposed functional form for B is

$$B = \frac{q}{C_0} \tag{11}$$

where q is a constant to be determined from experimental data. As in the case of Equation 10, the functional form in Equation 11 will need to be justified later using appropriate experimental data. In concluding this section it is noted that Equation 4 combined with Equations 10 and 11 provides the required functional forms for analyzing experimental data for moisture breakthrough time in the accelerated tests involving different temperature and humidity conditions. As expected, the proposed functional form suggests that, as absolute humidity C_0 decreases, the breakthrough time of the edge seal tends to infinity, and that, as temperature increases, the breakthrough time of the edge seal decreases. Both of these relationships are preserved while the quadratic dependence of breakthrough time on width of the edge seal is maintained.

Experimental set-up, results and analysis

In previous product-level testing for moisture ingress at MiaSolé, $CoCl_2$ impregnated paper (Micro Essentials Laboratory, Hydrion Humidicator Cat. No. HJH-650) was used as an indicator on various glass/glass module constructions (see Fig. 1(b)). Breakthrough was determined to be the point at which the paper turned from its blue anhydrous state to one of its hydrated-state colours. However, even with edge seal widths of approximately 3–4mm (dimensions at which reasonable precision can be maintained in a typical glass/glass structure), most experiments with desiccated edge seals tended to

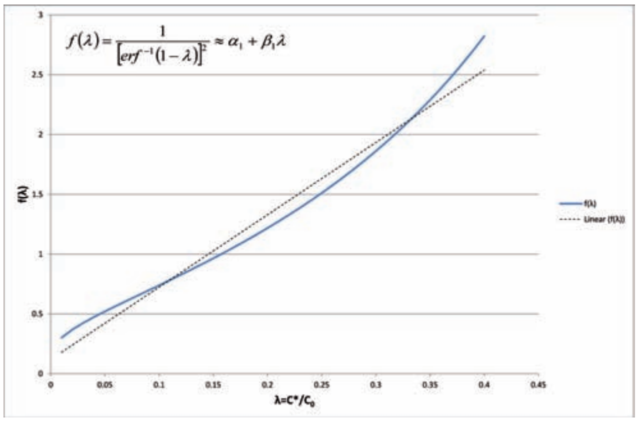

Figure 2. Approximation used in Equation 9.

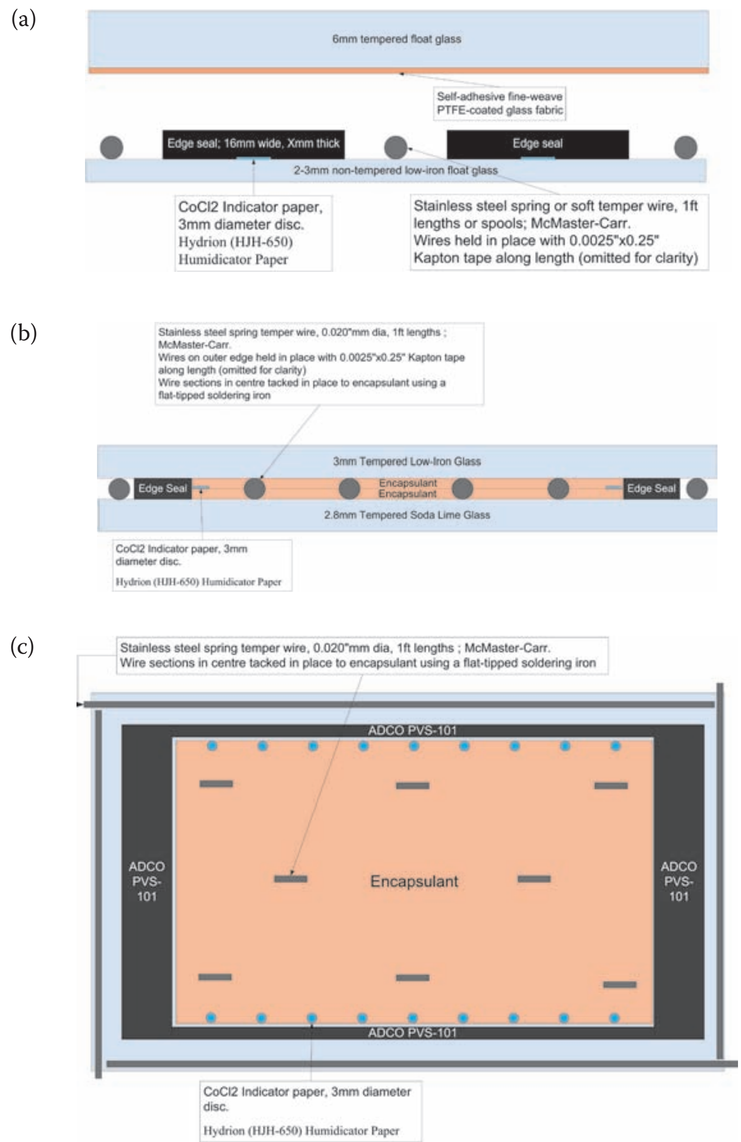

Figure 3. Sample construction for accelerated testing: (a) Type I samples; (b) Type II samples; (c) Planar view of Type II samples.

take in excess of 2000hrs at 85°C/85%RH to reach the breakthrough point. The 85°C/85%RH condition is one of the most aggressive conditions that can be controllably managed in available environmental chambers. In order to test a wider range of conditions to validate modelling parameters, it is necessary to extend the experimental conditions to lower acceleration factors. This, along with the time factor, renders the use of only glass–glass samples unfeasible.

> "Most experiments with desiccated edge seals tended to take in excess of 2000hrs at 85°C/85%RH to reach the breakthrough point."

Two types of samples were therefore prepared for testing based on the experimental set-up described earlier:

1. Type I samples: plaques with a thin layer of edge seal material (~1mm) applied to the glass, and moisture indicator paper ($CoCl_2$ impregnated paper) against the glass. See Figs. 3(a) and 4(a).

2. Type II samples: glass–glass mini-modules with narrow edge seal (~3mm), encapsulant and moisture indicator paper ($CoCl_2$ impregnated paper). See Figs. 3(b), 3(c) and 4(b).

The first type of sample – Type I – facilitates sub-1mm path lengths, which result in testing times reduced by an order of magnitude. In order to address potential convolution from interfacial diffusion along the edge seal and glass interface in the glass–glass edge seal structure, a second type of sample – Type II – was constructed, and data from overlapping path lengths were shown to be equivalent. Samples of Type I provide quick turnaround in terms of moisture penetration results for smaller dimensions, while samples of Type II are consistent with a typical module construction.

Type I samples

Fig. 3(a) shows the Type I sample construction. The sample consists of using indicator paper on the glass with the edge seal material directly above it. The width of the edge seal material (see cross section in Fig. 3(a)) is significantly greater than its thickness above the indicator paper, thereby ensuring that the primary path (shortest) of moisture diffusion to the indicator paper is through the thickness of the edge seal material above it. The sample is constructed using 3mm discs of moisture paper, and dispensing edge seal material onto it, with the whole structure supported on glass. Compression of the edge seal during lamination was achieved through the use of a tempered glass plate (6mm soda lime glass, 305mm × 205mm) to which a thin self-adhesive PTFE fibreglass fabric had been attached as a release layer. Lamination was carried out in a standard laboratory-scale flatbed vacuum laminator. The process set-points were as follows: platen temperature = 160°C, vacuum time = 6min (pressure at less than 100Pa after 1min), transition to full atmospheric press = 1min, and press time = 8min. Precise control of the edge seal thickness was achieved through the use of precision-formed stainless steel wire (McMaster-Carr) as spacers set between the test sections. The spacers were held in place with high-temperature ¼" × 0.0025" Kapton tape (McMaster-Carr 7648A71 and 7648A711). The placement of these spacers is illustrated in Fig. 3(a) and also in Fig. 4(a). The use of 2mm-thick (305mm × 205mm) non-tempered glass as the sample support allowed simple cross-sectioning, confirming the thickness of the edge seal over the indicator paper. For these samples, one platen had several moisture indicator discs (36 per platen). There were two such platens tested per chosen condition.

Type II samples

Figs. 3(b) and (c) show the glass–glass sample construction (Type II) for the accelerated testing of edge seal material; this sample structure more closely represents that of a typical module. However, because of variations in glass thickness and the encroachment of encapsulant into the edge seal, the path length variability can be higher than for the thin layer samples. In order to minimize the path length variation, a method was developed to control the compression of the edge seal/encapsulant structure. This consisted of wire spacers placed at the edges of the glass samples as well as small (5–10mm long) pieces of wire placed in the encapsulant to act as hard stops for the compression of the glass during lamination. The thickness of the spacers/edge seal was chosen such that the edge seal was allowed to compress a minimum of 20% of its thickness to ensure proper wet-out of the glass. The initial width of the edge seal in the test area was determined through experimentation to produce the desired final path length after lamination for the various samples. The path lengths for actual tested samples were confirmed by cross-sectioning right next to the indicator paper disc locations.

In both cases (Type I and Type II samples), breakthrough time is characterized by the detection of the onset of colour change of the moisture indicator paper described earlier. Fig. 4 shows representative images of two types of sample.

It follows from Equations 4, 10 and 11 that the goals of the experimental design are to:

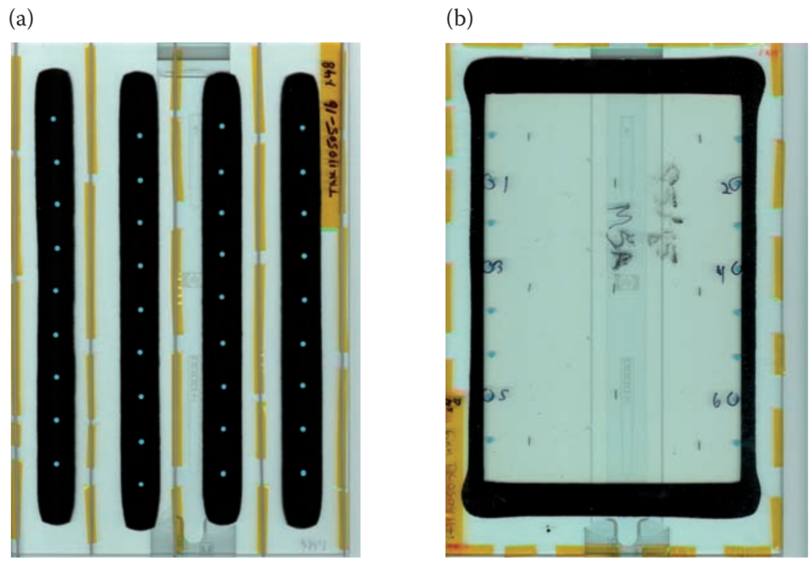

Figure 4. Laminated sample with thickness/width of the edge seal material controlled by SST wires used as spacers: (a) representative Type I sample; (b) representative Type II sample.

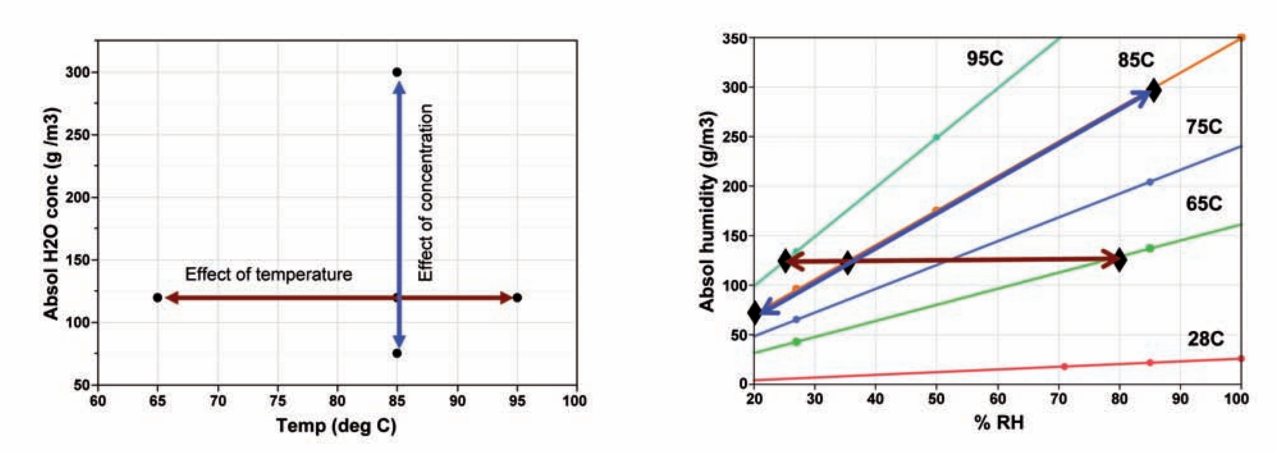

Figure 5. Test conditions chosen in accelerated testing in terms of temperature and concentration and equivalent representation in terms of temperature and relative humidity.

1. Validate the form of Equation 4, which describes a quadratic dependence of breakthrough time on edge seal width.

2. Validate the form of Equations 10 and 11 and demonstrate that the factor A exhibits Arrhenius dependence on temperature and that factors A and B exhibit hyperbolic dependence on moisture concentration.

3. Determine the parameters α, β, γ and q.

These goals can be accomplished by choosing experimental conditions such that the effects of concentration and temperature, associated with functional forms described in Equations 10 and 11, are evaluated independently of each other. An orthogonal experimental design was employed, wherein three temperatures are used at a given concentration and three concentrations are used at a given temperature, with a common temperature and concentration. The next question relates to the choice of the concentration and temperature levels. The considerations and constraints include:

- The degree of acceleration should allow a practical test duration.

- Over the range of chosen conditions, the materials should be expected to behave in a similar fashion to that for conditions encountered in field deployment.

- Environmental chambers should be able to maintain the set conditions, which precludes extreme temperature and relative humidity conditions.

- It should be possible to fabricate and measure edge seal path lengths dictated by the experimental conditions/durations.

At the outset, data for similar materials from Kempe et al. [6] were used to estimate breakthrough times for different conditions. When all the considerations and constraints were taken into account, the test conditions shown in Fig. 5 were arrived at. Finally, the temperature and moisture conditions were then translated into temperature and relative humidity conditions to accommodate the conventional way of setting up environmental chambers.

The change in colour of the indicator paper was monitored by scanning the sample on a flatbed system and by visual inspection. A colour change relative to the baseline was taken as an indication of moisture breakthrough. The colour change was monitored by inspections every 24hrs for the first 360hrs of exposure. One of the limitations of the approach presented here for monitoring is that opening and closing the chamber for inspection introduces delays owing to the time taken by the chamber to reach equilibrium after inspection. Because of this, the resolution of time to failure is limited to ±12hrs, which is a significant limitation for samples of small thickness. The frequency and time of inspection was adjusted based on estimated breakthrough times as more data became available, but this never exceeded 72hrs, and, in some instances of small-thickness samples, the measurements were repeated. Whenever there was an uncertainty in breakthrough time because of colour change between two inspections, the mid-point of the two times was chosen as the time to failure. In some cases the colour change approximately coincided with the inspection times and was recorded accordingly. In short, based on the inspection schedule that was practical, the best estimate of time for change of colour was chosen as the breakthrough time. Typically, all of the indicator paper discs changed colour within the sample in a single 24hr inspection interval. This limited our ability to understand the statistical variation within the samples. However, the colour change was found to be consistent across the entire platen in all of the observations, which therefore established the consistency of the breakthrough time for the group of data points.

"The proposed functional forms show a very good fit to the experimental data."

Figs. 6(a) and 7(a) show the results obtained from accelerated tests conducted in this manner. Each data point on these plots represents the average thickness over a number of discs for that condition and the breakthrough times as observed by the onset of colour change. As can be seen, the proposed functional forms show a very good fit to the experimental data. The corresponding constants (fit parameters) have also been extracted from these fits and are shown in Figs. 6(b), 7(b) and 7(c).

Prediction of field performance

This section addresses the question of incorporating varying ambient conditions in order to predict field performance of edge seal material using results from accelerated testing. The variation of ambient conditions (T, RH) essentially results in the variation of edge concentration, C_0, as a function of time for a given edge seal configuration, and the variation of

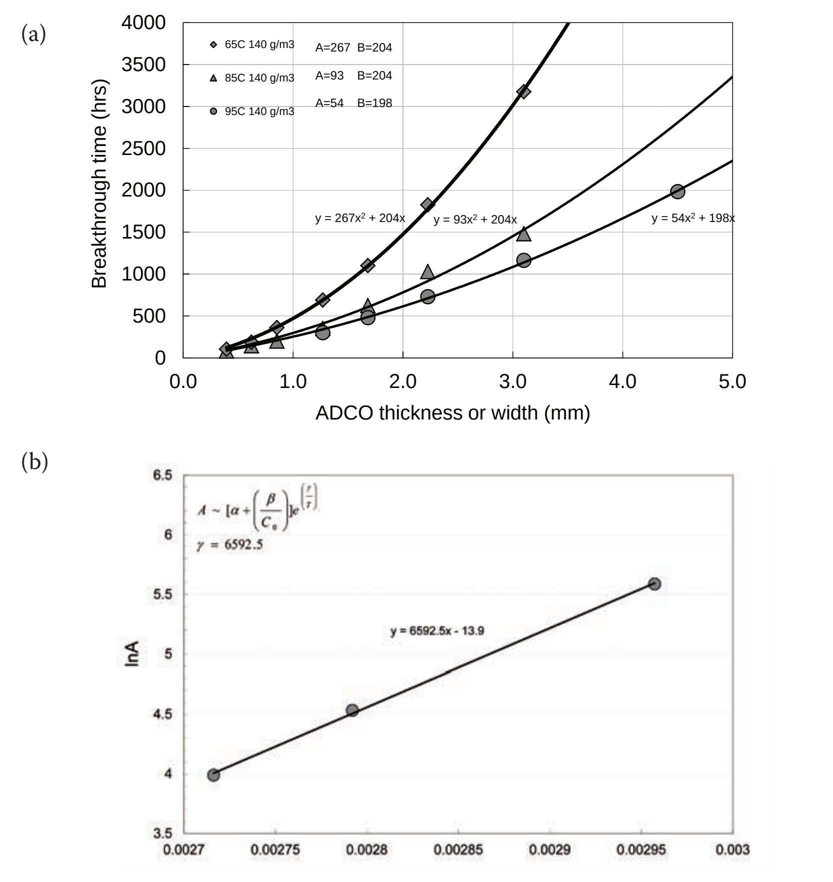

Figure 6. Experimental results of varying temperature at constant absolute humidity: (a) demonstration of quadratic variation of breakthrough time with width; (b) obtaining the Arrhenius variation for constant A.

diffusion coefficient, D, as a function of temperature (which in turn changes as a function of time). It is instructive to consider first the effect of temporal variation in diffusion coefficient. In this case Equation 1 can be written as

$$\frac{\partial C}{\partial t} = D(t)\frac{\partial^2 C}{\partial x^2} \tag{12}$$

The solution to this diffusion equation for the 1D case may be obtained by introducing a new transformation variable

$$\tau = \int_0^t D(\xi)d\xi \quad \Rightarrow \frac{\partial C}{\partial \tau} = \frac{\partial^2 C}{\partial x^2} \tag{13}$$

and is given by

$$C(x,t) = \mathrm{C}_0\left[1 - erf\left(\frac{x}{2\sqrt{D_{\mathrm{eff}}t}}\right)\right] \tag{14}$$

where

$$D_{\mathrm{eff}} = \frac{1}{t}\int_0^t D(\xi)d\xi \tag{15}$$

Note that for a time sufficiently long, a practical approximation to this result for the case in question may be obtained by carrying out the integral in Equation 15 over a representative period of variation, such as a typical meteorological year (TMY). The solution given by Equation 14 holds for the special case of edge concentration remaining constant over the period of interest.

The effect of time-varying the edge concentration can be examined separately. Assume that the period of variation of edge concentration is small (daily) compared with the diffusion time (expected breakthrough time of several years). To examine how far into the edge seal the time variations of the edge concentration will have a significant effect, the problem defined by the following equation can be considered

$$\frac{\partial C}{\partial t} = D\frac{\partial^2 C}{\partial x^2} \tag{16}$$

with the conditions

$$C(0,t) = \mathrm{C}_0 \sin \omega t \qquad C(x \to \infty, t) = 0 \tag{17}$$

It can be shown that the solution to the problem represented by Equations 16 and 17 is given by

$$C(x,t) = \mathrm{C}_0 \exp\left[-\left(\sqrt{\frac{\omega}{2D}}\right)x\right]\sin\left(\omega t - \left(\sqrt{\frac{\omega}{2D}}\right)x\right) \tag{18}$$

It is seen that, because of the exponential pre-factor, the oscillations of edge concentration with time are damped out within a short distance into the edge seal. For $\omega = (2\pi/24)\mathrm{hr}^{-1}$ and a representative diffusivity value of $0.2\mathrm{mm}^2/\mathrm{hr}$, the associated length scale is given by $l \approx \sqrt{(2D/\omega)} = 1.2\mathrm{mm}$ for decay by $\exp^{-1}$, i.e. a reduction to 36% of the outside amplitude. Typical edge seal widths in PV modules are an order of magnitude larger (~10mm) and hence, for practical purposes, an average concentration at the edge may be considered for this analysis. Note that seasonal variations (period ~3 months) may manifest themselves at a fraction of external amplitudes at the inner edge of the edge seal. However, in the case of PV modules, it is common to use edge seals loaded with desiccants as pointed out earlier. Hence, the magnitude of variations at the inner edge of the edge seal, even for seasonal variations, is not expected to be significant until the desiccant in the edge seal is consumed. On the basis of these considerations, an average concentration over a TMY was used for the analysis.

"Oscillations of edge concentration with time are damped out within a short distance into the edge seal."

From the discussion above and the results in Equations 14, 15 and 18, the following methodology is proposed for predicting field performance of edge seal materials tested:

1. Obtain the breakthrough time in various tests in standard temperature- and humidity-controlled chambers.
2. Determine the fit parameters A, B and γ given by Equations 10 and 11, as shown in previous sections. This involves obtaining the fit parameters α, β and q in Equations 10 and 11.
3. Establish the average absolute humidity for a given location using TMY data.
4. Work out an equivalent temperature for a location using TMY data from

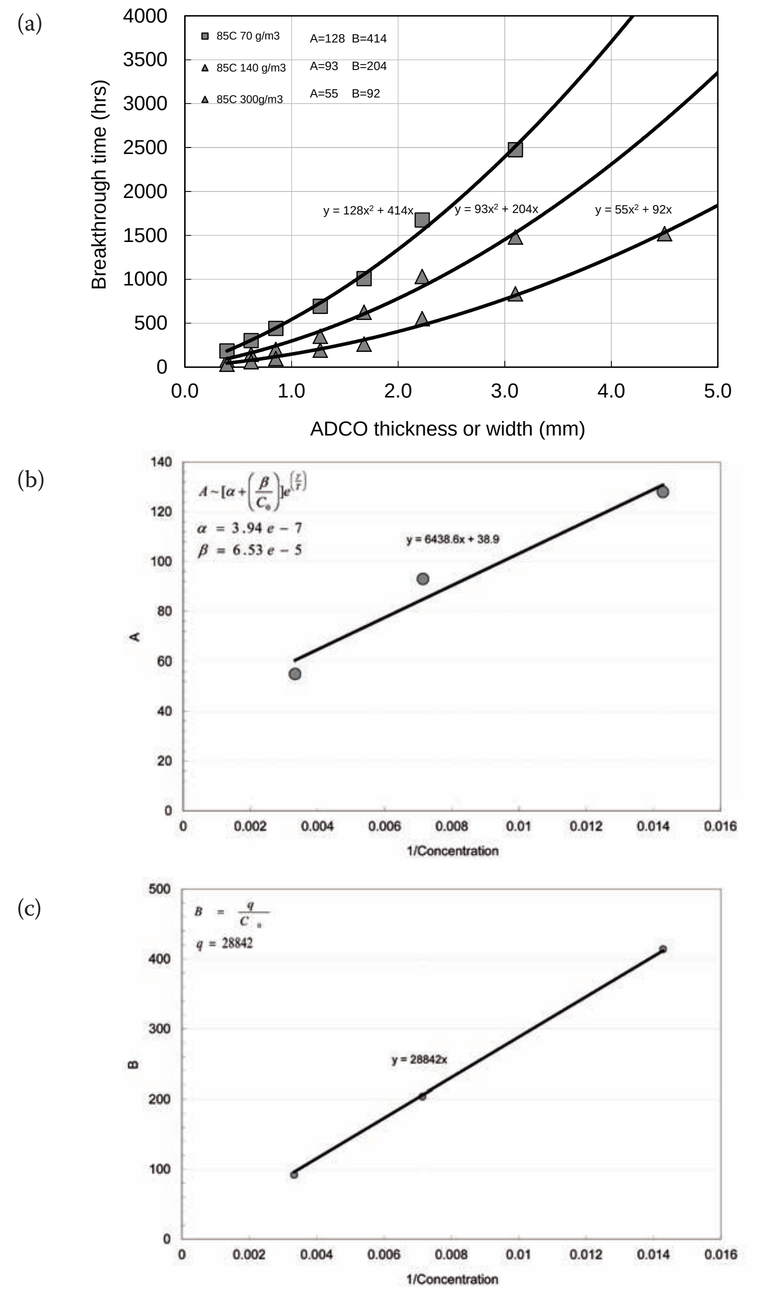

Figure 7. Experimental results of varying absolute humidity at constant temperature: (a) demonstration of the proposed quadratic variation of breakthrough time with width; (b) obtaining the fit parameters α and β; (c) obtaining the fit parameter q.

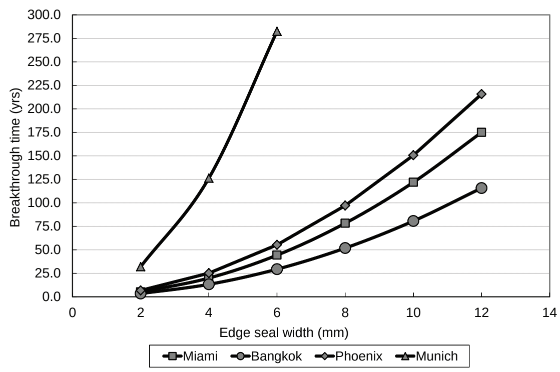

Figure 8. Predicted edge seal moisture breakthrough time for a particular edge seal used in certain MiaSolé glass–glass modules at selected locations.

$$\exp\left(-\frac{\gamma}{T_{eq}}\right)=\frac{1}{t_{1yr}}\int_0^{t_{1yr}}\exp\left(-\frac{\gamma}{T(t)}\right)dt \tag{19}$$

where the integral is performed over a typical year. An option to improve upon this estimate of T_{eq} is to use models validated by correlation to field data and to use $T(t)$ as the module temperature for given ambient conditions in the TMY data, rather than using the ambient temperature directly.

5. Calculate A and B for field conditions.

6. Substitute these values for A and B in Equation 4 to predict the field breakthrough time of the edge seal material at a given location.

Using the above approach, edge seal breakthrough time has been predicted for a particular case of edge seal used in certain MiaSolé glass–glass modules. These predictions are given in Fig. 8: it is seen that the predicted edge seal lifetime with edge seal width ~10mm is far beyond the intended service lifetime, even for hot and humid locations.

"In a particular case of edge seal, it was established that moisture ingress can be prevented well beyond the intended service lifetime."

Conclusion

The purpose of this work has been to provide a theoretical framework, an experimental technique for accelerated testing, and a method consistent with the theory for assessing edge seal field performance in a way that is decoupled from other components in a PV module. A theoretical framework was developed using an analytical solution to the 1D diffusion equation and observations of the mathematical characteristics of associated functional forms. This enabled functional forms to be proposed for the variation of breakthrough time (moisture penetration) with given edge seal width under different ambient or chamber conditions. A relatively inexpensive test technique was developed such that the tests can be conducted in standard environmental chambers used for product level testing. Proposed functional forms were validated by experimental data from accelerated testing. A methodology based on the developed theoretical framework was provided for predicting field performance of the edge seal from the results of accelerated testing. In a particular case of edge seal used in certain MiaSolé glass–glass modules, it was established that moisture ingress can be prevented well beyond the intended service lifetime, even for the most aggressive climate conditions evaluated.

References

[1] U.S. Photovoltaic Manufacturing Consortium (PVMC) 2013, "U.S. CIGS photovoltaic roadmap", July.

[2] Pern, J. 2008, "Module encapsulation materials, processing and testing", APP Int. PV Reliab. Worksh., Shanghai, China.

[3] Livingston, H. "SSB-1: Guidelines for using plastic encapsulated microcircuits and semiconductors in military, aerospace and other rugged applications", Report, Solid State Dev. Comm. Gov. Electron. Inf. Tech. Assoc. (GEIA).

[4] Shirley, C.G. 1994, "THB reliability models and life prediction for intermittently-powered non-hermetic components", *Proc. 32nd Ann. Int. Reliab. Phys. Symp.*, San Jose, California, USA, pp. 72–77.

[5] Coyle, D.J. 2013, "Life prediction for CIGS solar modules part 1: Modeling moisture ingress and degradation", *Prog. Photovolt.: Res. Appl.*, Vol. 21, pp. 156–172.

[6] Kempe, M.D. et al. 2010, "Evaluation and modeling of edge-seal materials for photovoltaic applications", *Proc. 35th IEEE PVSC*, Honolulu, Hawaii, USA.

[7] Otth, D.H. & Ross R.G. 1983, "Assessing photovoltaic module degradation and lifetime from long term environmental tests", *Proc. 29th Inst. Env. Sci. Ann. Meet.*, pp. 121–126.

[8] Osterwald, C.R. & McMahon, T.J. 2008, "History of accelerated and qualification testing of terrestrial photovoltaic modules: A literature review", *Prog. Photovolt.: Res. Appl.*, Vol. 17, No. 1, pp. 11–33.

[9] Hallberg, O. & Peck, D.S. 1991, "Recent humidity accelerations, a base for testing conditions", *Qual. Reliab. Eng.*, Vol. 7, pp. 169–180.

[10] Peck, D.S. 1986, "Comprehensive model for humidity testing correlation", *Proc. IRPS*, pp. 44–50.

[11] Peck, D.S. 1970, "The design and evaluation of reliable plastic encapsulated semiconductor devices", *Proc. IRPS*, pp. 81–93.

[12] Rasal, R.M. & Snowwhite, P.E. 2010, "Solar edge sealants with a better balance of properties", Poster Session, PV Mod. Reliab. Worksh., Denver, Colorado, USA.

[13] Crank, J. 1975, *The Mathematics of Diffusion*, 2nd edn, Oxford: Oxford University Press.

About the Authors

Kedar Hardikar is a staff scientist at MiaSolé and holds a Ph.D. from the Division of Engineering, Brown University. His roles at MiaSolé include assisting product development, improving reliability of the product, and leading selected research and development projects using analysis and computational models. An author of several technical publications, Kedar held several key positions over a period of more than 10 years in the semiconductor capital equipment industry and in the consumer electronics industry before joining MiaSolé.

Dan Vitkavage holds a Ph.D. in chemistry from the University of North Carolina at Chapel Hill. He has authored numerous technical publications and presentations and is the holder of 18 US patents. Dan has held a range of technical and management positions within the semiconductor industry, both in the area of IC fabrication and in PV. He is currently a senior director of technology for Lam Research Corporation.

Ajay Saproo is the director of reliability and process integration at MiaSolé. He is responsible for ensuring product performance and reliability, including the development of tests and solutions relating to reliability problems, technology qualification, product certification, lifetime models and field validation. Ajay holds an M.S. in electrical engineering from the University of Cincinnati.

Todd Krajewski is the process development manager for flexible modules at MiaSolé. He holds a bachelor's degree in chemistry and is a co-inventor on 10 issued patents and numerous patent applications. Todd's focus has been on polymer synthesis, ultra-barrier films and material integration in the semiconductor, OLED and solar fields.

Enquiries

Kedar Hardikar
MiaSolé
2590 Walsh Ave
Santa Clara, CA 95051
USA

Tel: +1 408 919 5702
Email: khardikar@miasole.com